Nanoscale Advances

ROYAL SOCIETY OF CHEMISTRY

PAPER

View Article Online
View Journal | View Issue

Cite this: *Nanoscale Adv.*, 2020, **2**, 2986

Thermally induced intra-molecular transformation and metalation of free-base porphyrin on Au(111) surface steered by surface confinement and ad-atoms†

Dipayan Sen, [a] Piotr Błoński, [a] Bruno de la Torre, [ab] Pavel Jelínek[ab] and Michal Otyepka *[a]

We investigated chemical transformations of a fluorinated free-base porphyrin, 5,10,15,20-tetrakis(4-fluorophenyl)-21,23*H*-porphyrin (2H-4FTPP) under a Au(111) surface confinement and including gold adatoms by using an experiment and density functional theory based first-principles calculations. Annealing of 2H-4FTPP led to cyclodehydrogenation of the molecule to a π-extended fused aromatic planar compound, 2H-4FPP, and metallation of the porphyrin ring by Au atoms to Au-4FPP complex. Noticeable lowering of bond-dissociation energies of the pyrrole's C–H bonds of the Au(111) supported molecule with respect to their values in the gas phase explained the observed on-surface planarization. Our findings also indicate that Au adatoms may catalyze cleavage of C–H/F bonds in temperature-initiated processes on Au surfaces. BDEs and explicit inclusion of Au adatoms helps to rationalize thermally induced chemical reactions on the respective surface.

Received 23rd March 2020
Accepted 26th May 2020

DOI: 10.1039/d0na00401d

rsc.li/nanoscale-advances

Introduction

The recent developments in on-surface synthesis enable the construction of tailored covalent nanostructures under ultra-high vacuum (UHV) conditions on metal surfaces which are unattainable in solution.[1–3] Moreover, the capability of acquiring submolecular imaging using scanning probe microscopy (SPM) with functionalized probes[4,5] provided the unique method to determine intermediates and final products of on-surface reactions.[6] The on-surface synthesis inherently taking place on a metal surface poses many fundamental questions, *e.g.*, to what extent the surface confinement *i.e.*, either a physical or chemical adsorption, may affect studied chemical processes? Furthermore, the on-surface chemical processes examined by UHV-SPM are usually thermally induced, which opens another question: since it is well known that metal atoms may detach from edges of terraces and move on the surface as adatoms[7] and such adatoms do not have saturated valences, may they represent spots enabling catalysis of the surface chemical reactions?

Despite the unprecedented chemical resolution provided by the high-resolution SPM technique, we still lack detailed understanding of reaction mechanisms due to limited temporal resolution. The reaction mechanism is hence deduced from the identified intermediates and reaction products.[8] Theoretical calculations help to search for an optimal reaction pathway.[9–13] In order to follow the real processes happening during on-surface chemistry, the involvement of the catalytic adatoms has to be explicitly considered.

Porphyrins belong to a class of molecular systems that already demonstrated key utility in diverse fields ranging from catalysis, spintronics, molecular sensing and photosynthesis to biological applications such as metabolism.[14,15] Such high potential of porphyrin molecules thus enthused researchers to pursue investigations on porphyrin derivatives and their self-assembly. Controlling chemical reactions of surface restricted porphyrin molecules by rational designing could open up a plethora of prospective research avenues including modifications of the physicochemical properties of surface-confined porphyrin derivatives *in situ* by macrocycle metalation.[16–18] However, to realize its potential to the fullest, an in-depth understanding of the various conformations of the concerning species at the atomic level is necessary, which is unfortunately still largely lacking. In the current work we addressed (i) the chemical evolution of the fluorinated free-base porphyrin under surface confinement on Au substrate and (ii) the catalytic role of gold adatoms on Au(111) in the 2H-4FTPP → 2H-4FPP → Au-4FPP transformation by combining UHV-SPM experiments and density functional theory (DFT) computations. Our results indicate that the gold adatom significantly affected the reaction

[a]*Regional Centre of Advanced Technologies and Materials, Faculty of Science, Palacký University, Olomouc, Czech Republic. E-mail: michal.otyepka@upol.cz*

[b]*Institute of Physics, Academy of Sciences of the Czech Republic, Prague, Czech Republic*

† Electronic supplementary information (ESI) available. See DOI: 10.1039/d0na00401d

barriers of various processes thus modulating the reaction mechanism. Generally, a role of catalytic adatoms has to be carefully analysed in order to obtain plausible reaction mechanism of on-surface catalysed processes.

Methods

Computational details

DFT based first principles computations were carried out by using Vienna *Ab initio* Simulation Package (VASP)[19,20] which incorporates projector-augmented-wave (PAW) method[21,22] along with plane wave basis sets with an energy cut-off of 500 eV. Electronic exchange and correlation effects were treated by using Perdew–Burke–Ernzerhof (PBE) exchange–correlation functional within the generalized gradient approximation (GGA).[23] All computations were performed in spin unrestricted manner. Zero damping DFT-D3 method of Grimme[24] was utilized in all computations to account for the dispersion corrections. Brillouin zone samplings were kept restricted to Γ point only due to the supercell dimensions being sufficiently large.

The Au(111) surface was modelled by using 7 × 7 and 8 × 8 supercells consisting of 4 Au layers of which the bottom two layers were kept constrained in all structural relaxations. Vacuum layer of length ∼12 Å was deployed along the off-planar direction to ward off spurious interactions with the periodic images. Bare Au(111) substrate (cell parameters and the internal atomic positions), the Au(111) slab with pre-adsorbed Au adatom (the internal atomic positions), freestanding fluorinated free-base porphyrin, 2H-4FTPP, molecular model (the internal atomic positions) and the 2H-4FPP/Au(111) heterostructures (the internal atomic positions) were relaxed until all forces were reduced to less than 0.01 eV $Å^{-1}$. Their respective total energies and electronic properties were re-computed using PBE0 hybrid functional[25] (*i.e.*, by mixing the PBE exchange energy and Hartree–Fock (HF) exchange energy in 3 : 1 ratio, along with the full PBE correlation energy). Partial charges of various atomic species were computed by Bader analysis.[26] The VASP data (for selected configurations) were also compared against non-periodic DFT results performed by using Gaussian code[27] and B3P86 hybrid functional[28] (which uses the P86 correlation functional instead of LYP but retains the three parameters derived for B3LYP[29]).

Relative stabilities of various surface-adsorbed species (*i.e.*, Au adatom on an Au(111) slab and the 2H-4FPP (bis-(2,10-difluoro-5*H*-diindeno[2,1-*b*:1′,2′-*d*]pyrrole)-5,7-bis(1*H*-pyrrol-2-yl)) molecule on a bare Au(111) slab and the Au(111) slab with pre-adsorbed Au adatom) were obtained from their adsorption energies, E_{ads}, calculated using the following expression:

$$E_{ads} = E_{tot} - E_{slab} - E_{adsorb}, \quad (1)$$

where E_{tot} represents the total energy of the entire surface-adsorbed system, E_{slab} is the total energy of the Au(111) slab, and E_{adsorb} is the total energy of the gas-phase 2H-4FTPP or the free Au atom. Lower value of E_{ads} implies higher energetic stability of the surface-adsorbed system.

The H and F bond dissociation energies of the 2H-4FTPP molecule were computed by using the following formula:

$$BDE = E_{dis} + E_{H/F} - E_{2H\text{-}4FTPP} \quad (2)$$

where E_{dis} is the total energy of the 2H-4FTPP molecule with a broken H/F bond (both in the gas-phase and adsorbed on the Au(111) substrate), $E_{H/F}$ is the total energy of an isolated H and F atom, and $E_{2H\text{-}4FTPP}$ represents the total energy of an intact 2H-4FTPP molecule (or 2H-4FPP plus the Au(111) slab for the heterostructures).

Experimental details

The experiments were performed with an ultra-high vacuum combined noncontact-AFM/STM system (Createc) at 5 K using a qPlus sensor equipped with a Pt/Ir tip, where the base pressure was below 5 × 10^{-10} mbar. The Au(111) substrate was prepared by standard cycles of Ar^+ sputtering and subsequent annealing. 2H-4FTPP species are commercial from Porphyrin Systems and were sublimated from a tantalum pocket onto a clean Au(111) at room temperature. Next, samples were transferred to the SPM stage held at 5 K. In nc-AFM imaging, a metal tip mounted onto a qplus sensor (resonant frequency ≈ 30 kHz; stiffness ≈ 1800 N m^{-1}) was oscillated with a constant amplitude of 50 pm. The tip apex was functionalized by a CO-molecule picked up from Au(111) substrate. All images were taken at a constant height mode.

Results

Experimental findings

Fig. 1a shows the free-base porphyrin 2H-4FTPP used in this study. Deposition of small amount of molecules on the Au(111) substrate at room temperature led single 2H-4FTPP featuring a two-fold symmetric characteristics attributed to the nonplanar macrocycle deformation of the porphyrin upon surface stabilization as depicted in Fig. 1b. High-resolution AFM image clearly shows the saddle shape deformations attributed to the twisted fluorine-aryl moieties whereas the inner depression is assigned to the free-base macrocycle (Fig. 1b). After annealing to 500 K and 575 K molecular chains stabilized by intermolecular C–H⋯F–C interactions confined to fcc regions of the Au(111) herringbone reconstruction are observed. Fig. 1c shows that thermal annealing of the sample to 575 K gave rise to the formation of one-dimensional supramolecular arrays, stabilized by weak intermolecular interactions.

High-resolution AFM images (Fig. 1b and c) unambiguously show that the 2H-4FTPP molecules underwent planarization through dehydrogenation and electrocyclic ring closure of their aryl termini and macrocyclic pyrroles, *i.e.*, 2H-4FTPP → 2H-4FPP. Note, that the first annealing step at 500 K planarized the fluorinated porphyrin precursor but preserved the integrity of the macrocycle and its C–F bonds. Regarding of featuring the macrocycle, both constant height high-resolution STM and AFM images display up to three different planarized species, to be termed A, B and C which are assigned to non-metallated, Au-adatom metallated (AuB-4FPP) and Au-surface metallated

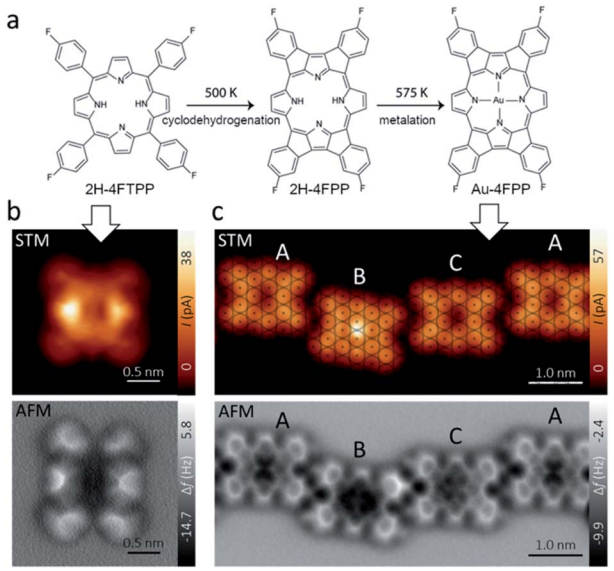

Fig. 1 (a) Chemical sketch of thermal-assisted reaction pathway of 4F-TPP on Au(111) affording: planarization of the molecular backbone *via* cyclodehydrogenation and electrocyclic ring closure and self-metallation with an Au atom from Au(111) surface. (b) Constant height STM (top) and AFM (below) images with functionalized CO-tip of a single 2H-4FTPP molecule after adsorption on Au(111) at RT. (c) Constant height STM (top) with superimposed atomic register of Au(111) substrate and AFM (below) images of A (non metallated), B (adatom-metallated) and C (surface-metallated) types of 2H-4FPP molecules after annealing to 575 K.

(AuC-4FPP) molecules, respectively. The second annealing step at 575 K for 30 minutes induced self-metalation in approximately 20% of the planarized molecules. Statistically we found approximately 65% of A molecules, 20% of B and 15% of C type. Molecule A shows a void at the core in both STM and AFM images as expected for empty macrocycles. On the other hand, on molecules B and C, a cross-shaped feature is visible in the AFM images, a similar contrast as has also been observed on other metal phthalocyanines and porphyrins.[30,31] Interestingly, significant differences are clear in STM images of molecules B and C. The former one displays a fain protrusion at the core whereas a void is featured at the latter one. This observation points to a two different metallation mechanism in B and C molecules. One shall note, that previous works on similar molecules have also reported intermediate metallated-states.[17,18] In fact, when we have a detailed look on the adsorption sites of the three species on Au(111) substrate with atomic resolution, we found significant differences (Fig. 1c top). The centre of molecule C was found to be close to top site, which allowed to develop coordination of the macrocycle with Au-surface atom, whereas, the centre of molecule A was found to be close to a bridge site so any Au atoms from the surface were too far to develop any coordination and localization of Au-adatoms is energetically unfavourable. In a different manner, the centre of B molecule was found close to a hollow site which is far from any surface atoms but energetically favourable for Au-adatom thus facilitating its coordination with the macrocycle.

Theoretical results

Preferred position of Au adatom on the Au (111) surface. To address the role of gold adatoms on Au(111) in the 2H-4FPP → Au-4FPP transformation, we first theoretically studied the adsorption of the Au adatom on the respective surface. The hollow fcc was found to be energetically most stable (E_{ads} = −69.62 kcal mol^{-1}) among adsorption sites examined for Au-adatom adsorption on the Au(111) surface shown in Fig. 2.

The stability of Au adatom in the hollow hcp site was marginally lower (E_{ads} = −67.91 kcal mol^{-1}). This was also reflected in the adatom-surface distance: 2.678 Å *vs.* 2.688 Å for Au in fcc and hcp hollow, respectively. The on-top and bridge positions were unstable, the Au adatom moved to the nearest hollow fcc site. Our results are in line with the combined experimental and theoretical work reporting the gold adatom located at a three-fold hollow site.[32] Test calculations by using a smaller 4 × 4 Au supercell and 4 × 4 × 1 *k*-point grid yielded E_{ads} = −70.17 kcal mol^{-1} at the adatom-surface distance of 2.684 Å for Au in the fcc hollow and E_{ads} = −68.87 kcal mol^{-1} at the adatom-surface distance of 2.695 Å for the adsorption in the hollow hcp.

Behaviour of 2H-4FTPP on the Au(111) surface. The 2H-4FTPP molecule adsorbed on the bare Au(111) surface at the distance of ∼3.2 Å to the Au topmost layer (E_{ads} = −124.9 kcal mol^{-1}) in a similar fashion as the structure in gas phase. Annealing at 500 K led to molecule planarization, *i.e.*, rotation of phenylene rings by ∼70° with respect to the conformation in the gas phase (Fig. 3a) and ring-closing (2H-4FPP, Fig. 3b). The final conformation of the adsorbate corresponds well to the experimental data (Fig. 1b) and is given by a balance between gain in adsorbate–surface interaction energy and deformation energy of the molecule. However, the formation of strong chemical bonds between 2H-4FPP and the Au(111) surface was not observed.

To rationalize the heat induced sequential intra-molecular transformations, (i) planarization of the molecular backbone *via* cyclodehydrogenation and electrocyclic ring closure (2H-4FTPP → 2H-4FPP), (ii) metallation with an surface Au atom

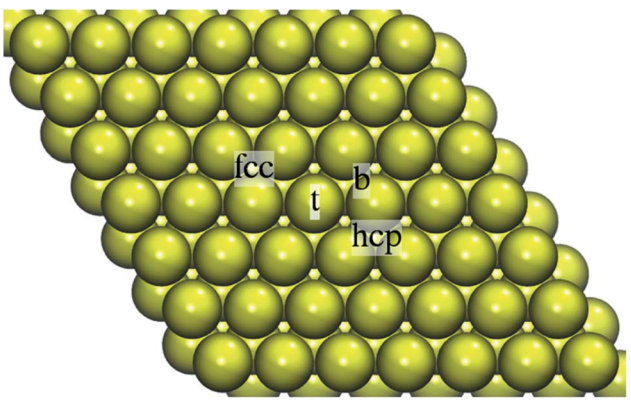

Fig. 2 Top view of the 7 × 7 4-layer slab representing the Au(111) surface with the on-surface adsorption sites indicated: on-top (t), bridge (b), hollow fcc, and hollow hcp.

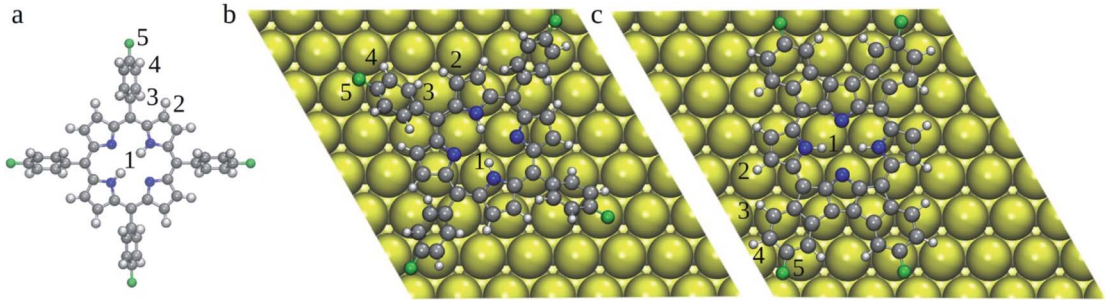

Fig. 3 Optimized 2H-4FTPP in the gas-phase (a) and 2H-4TFPP deposited on the Au(111) surface (top-view) (b). 2H-4FPP on Au(111) (c). Au atoms are shown in yellow, C in grey, N in blue, F in green, and H in white. BDEs of bonds labelled by numbers are gathered in Table 1.

(2H-4FPP → AuC-4FPP), we calculated BDEs of the relevant H (1–4) and F (5) atoms (Fig. 3) both of freestanding 2H-4FTPP and 2H-4FPP deposited on Au(111) (Table 1). It was shown that B3P86 provides good estimates of BDEs,[33,34] however, this functional was not implemented for periodic DFT calculations, therefore we tested performance of PBE0 + D3 against B3P86 functional. Both B3P86 and PBE0 + D3 provide the same orders of calculated BDEs and differ each other less than 3%, thus periodic DFT computations with PBE0 + D3 functional could reliably be deployed to study energetics and structural transformation of 2H-4FTPP → 2H-4FPP → Au-4FPP under surface confinement, a scope which falls outside of the purview of the non-periodic DFT implementations that are standard for standalone molecular models. C–F bond exhibited highest BDE, which implies, during chemical transformation induced by surface confinement or external stimuli, integrity of the fluorine functionalization is least likely to be perturbed. This observation directly corroborates the experimental observations.[35] The adsorption of 2H-4FTPP on the Au(111) surface led also to significant lowering of the H/F BDEs with respect to the gas phase (Table 1). Particularly the C–H_2 bond can be easily cleaved, which can lead to ring fusion at this particular C atom in agreement with the experimental observations.[35] The liberated H atoms will either bind to the Au surface or Au adatom (*vide infra*), and if two H atoms meet, they may form H_2, which would desorb to the gas-phase. However, atomic hydrogen can also passivate the defluorinated carbon atoms that do not participate in oligomers formation.[35] It should be noted that the surface confinement changed significantly order of BDEs, *i.e.*, susceptibility of individual bonds for reaction. The susceptibility of C–H_2 bond with respect to the vacuum can originate from the clash of H_2 and H_3 atoms caused by the rotation of phenyl ring due to molecule surface planarization. The barriers against the rotation of phenyl rings could be calculated by using Nudged Elastic Band method,[9] which however, will not be feasible for current systems. Therefore, here we have focused on rather simple indices (BDEs), which can be readily calculated even for large systems.

Behaviour of 2H-4FPP on the Au(111) surface with Au adatom. The 2H-4FPP molecule was initially placed on the Au(111) substrate in a way that the H/F bonds were in the vicinity of Au adatom that occupied hollow fcc, and the system was allowed to relax. The initial adsorption configurations are shown in the scheme to Table 2. The global minimum for the adsorption of 2H-4FPP corresponded to the GS adsorption site of Au adatom, *i.e.*, hollow fcc (1), on which the molecule was centred. The adsorption of 2H-4FPP centred on the Au adatom in hollow hcp was an energetically higher local minimum and was thus excluded from further considerations. The configurations in which the Au adatom bound to the rim positions (or in their close vicinity), also corresponded to the hollow fcc site of the Au adatom (34, followed by 2, 4 and 3), however were found to be energetically less stable. Furthermore, the 2H-4FPP molecule displayed some amount of bending while on the Au adatom (Fig. S2†), which may facilitate transition from rim positions to central position, and accordingly metalation of the molecule (Au^B-4FPP) in line with the experimental observations that demonstrated self-metalation in a comparable geometry.[35]

To further explore this point, we computed the BDEs of the relevant C(N)–H and C–F bonds of 2H-4FPP deposited on

Table 1 BDEs (in kcal mol^{-1}) of C(N)–H and C–F bonds labelled in Fig. 3. Relative values with respect to the lowest BDE are given in the bracket

	Freestanding	Freestanding	Au (111) adsorbed 2H-4FTPP	Au (111) adsorbed 2H-4FPP
Bond	B3P86	PBE0 + D3	PBE0 + D3	PBE0 + D3
N–H_1	111.8 (0.0)	111.8 (0.0)	143.3 (70.3)	95.8 (3.8)
C–H_2	124.5 (12.7)	121.8 (10.0)	120.1 (47.1)	92.0 (0.0)
C–H_3	119.3 (7.5)	116.2 (4.4)	74.0 (1.0)	97.2 (5.2)
C–H_4	121.5 (9.7)	117.7 (5.9)	73.0 (0.0)	95.9 (3.9)
C–F	129.9 (18.1)	127.8 (16.0)	127.6 (54.6)	105.5 (13.5)

Table 2 Adsorption energy (in kcal mol^{-1}) and relative adsorption energy (in parenthesis) of 2H-4FPP on Au(111) with pre-adsorbed Au adatom, whose positions relative to the relevant bonds in the molecule are indicated in the scheme above the table by orange dots. Au adatoms occupied fcc hollow in Au(111) (shown by the red dot), and the orientation of 2H-4FPP was accordingly adjusted. Selected final structures are shown in Fig. S2

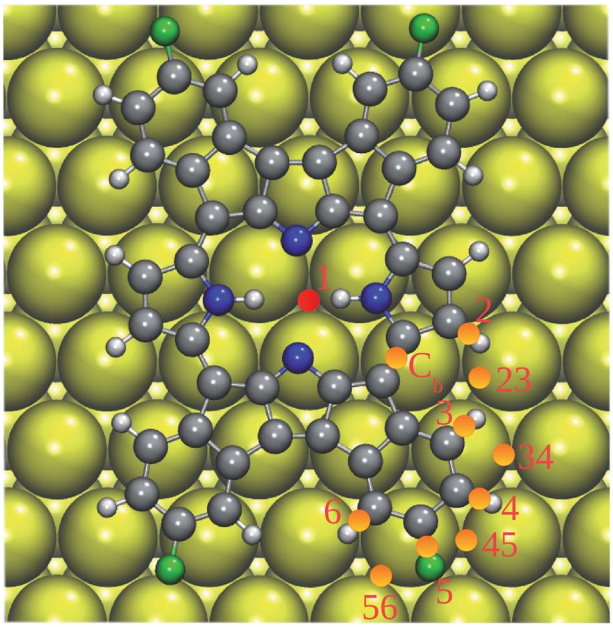

Position	E_{ads}	Position	E_{ads}
1_{fcc}	−133.4 (0.0)	4	−125.8 (−7.6)
1_{hcp}	−131.4 (−2.0)	34	−127.8 (−5.6)
C_b	−111.4 (−22.0)	5	−122.9 (−10.5)
2	−126.6 (−6.8)	45	−124.5 (−8.9)
3	−125.1 (−8.3)	56	−104.3 (−29.1)
23	−121.7 (−11.7)	6	−97.1 (−36.3)
Au(111)	−124.9 (−8.5)		

Au(111) with pre-adsorbed Au adatom. We used following notation: 1@Au1 for BDE of the N–H bond (1) of the central ring and Au adatom in the GS position (Au1), 2@Au23 for BDE of the C–H bond (2) and Au adatom in the rim position between two terminal H atoms (2 and 3), *etc.* The computed BDEs are listed in Table 3. The important point to note is that the Au adatom on the Au(111) surface changed BDEs of 2H-4FPP considerably. In the close proximity to the Au adatom, the drop in BDEs of the concerned bonds was most prominent. Conversely, if the Au adatom was located far away from the concerned bonds, their dissociation energies approached to that of them on the pristine Au(111) surface. Among all configurations considered, the central H atom(s) exhibited highest susceptibility to cleavage due to the Au adatom. This further supports the experimentally observed metallation of 2H-4FPP to Au-4FPP.[35]

Table 3 BDEs (in kcal mol^{-1}) of C(N)–H and C–F bonds of 2H-4FPP supported on Au(111) with pre-adsorbed Au adatom calculated with PBE0 + D3 (*cf.*, scheme to Table 2 and Fig. S2)

Configuration	BDE	Configuration	BDE
1@Au1	84.4	5@Au5	90.8
2@Au1	92.7	1@Au34	101.3
3@Au1	99.7	2@Au34	96.5
4@Au1	96.7	3@Au34	88.2
5@Au1	104.5	4@Au34	81.8
2@Au2	85.9	5@Au34	128.0
3@Au3	83.0	5@Au56	116.5
4@Au4	83.1	6@Au56	105.4

Bader charge analysis revealed an accumulation of $-0.046e$ on the Au adatom on the Au(111) surface. Conversely, for all configurations in which the Au adatom was at the nearest most stable position of the respective C(N)–H and C–F bonds of 2H-4FPP, it showed a small partial charge. Hence, a small electron transfer between the Au adatom and the molecule could be expected. Indeed, Fig. S3† displaying the charge-density-difference isosurfaces for these systems, confirmed the Au adatom donated electrons in all cases to 2H-4FPP. The charge transfer between Au and the molecule was significantly increased in the presence of adatom. The increased charge transfer between the Au adatom and the molecule and the Au–N bond-lengths (Fig. S4†) indicate on the formation of the respective chemical bonds.

Conclusions

In the current study we investigated the chemical evolution of the fluorinated free-base porphyrin (2H-4FTPP) under surface confinement on Au substrate and the catalytic role of gold adatoms on Au(111) in the 2H-4FTPP → 2H-4FPP → Au-4FPP transformation from both experimental and theoretical perspectives.

To rationalize the experimental findings, we investigated the energetics of 2H-4FTPP, 2H-4FPP, and metallated Au^{B}-4FPP configurations through DFT based first principle calculations. The obtained results readily indicated the H/F BDEs of the 2H-4FPP on the Au(111) surface are considerably lower in comparison to the same in gas phase. The pyrrole's C–H bond was found to be particularly vulnerable for cleavage which could explain the dehydrogenation and the subsequent planarization observed during experimental measures.

Various configurations of 2H-4FPP adsorbed on Au (111) with pre-adsorbed Au adatom were also investigated in detail. Among them, in direct agreement with experimental observations, a configuration in which the centre of 2H-4FPP rests on the Au adatom was found to be energetically most stable. Importantly, the Au adatom decreased BDEs of 2H-4FPP quite a considerably. The effect was most prominent for the bonds in direct vicinity to the Au adatom, thus conforming its catalytic role. Also, Bader charge analysis confirmed small amount of electron transfer between the Au adatom and the 2H-4FPP in these cases. These findings provided an atom-level insight into the mechanism of on-surface synthesis and transformation of porphyrin-derivative, and thus may stimulate the development of this emerging field.

Conflicts of interest

There are no conflicts to declare.

Acknowledgements

The authors gratefully acknowledge the support of the Operational Programme for Research, Development and Education of the European Regional Development Fund (Project No. CZ.02.1.01/0.0/0.0/16_019/0000754). MO acknowledges the ERC grant (683024) from the EU Horizon 2020 Research and Innovation Programme.

Notes and references

1 L. Grill, M. Dyer, L. Lafferentz, M. Persson, M. V. Peters and S. Hecht, *Nat. Nanotechnol.*, 2007, **2**, 687.
2 On-surface synthesis, *Proceedings of the International Workshop On-Surface Synthesis*, ed A. Gourdon, Springer, 2014.
3 S. Clair and D. G. de Oteyza, *Chem. Rev.*, 2019, **119**, 4717.
4 L. Gross, F. Mohn, N. Moll, P. Liljeroth and G. Meyer, *Science*, 2009, **325**, 1110.
5 P. Jelínek, *J. Phys.: Condens. Matter*, 2017, **29**, 343002.
6 D. G. de Oteyza, P. Gorman, Y.-Ch. Chen, S. Wickenburg, A. Riss, D. J. Mowbray, G. Etkin, Z. Pedramrazi, H.-Z. Tsai, A. Rubio, M. F. Crommie and F. R. Fischer, *Science*, 2013, **340**, 1434.
7 G. Antczak and G. Ehrlich, *Surface Diffusion: Metals, Metal Atoms, and Clusters*. Cambridge University Press, 2010.
8 A. Riss, A. Pérez Paz, S. Wickenburg, H.-Z. Tsai, D. G. De Oteyza, A. J. Bradley, M. M. Ugeda, P. Gorman, H. S. Jung, M. F. Crommie, A. Rubio and F. R. Fischer, *Nat. Chem.*, 2016, **8**, 678.
9 G. Henkelman and H. Jónsson, *J. Chem. Phys.*, 2000, **113**, 9901; *J. Chem. Phys.*, 2000, **113**, 9978.
10 J. Björk, *J. Phys.: Condens. Matter*, 2016, **28**, 083002.
11 M. Bieri, M.-T. Nguyen, O. Gröning, J. Cai, M. Treier, K. Aït-Mansour, P. Ruffieux, C. A. Pignedoli, D. Passerone, M. Kastler, K. Müllen and R. Fasel, *J. Am. Chem. Soc.*, 2010, **132**, 16669.
12 A. Lunghi, M. Iannuzzi, R. Sessoli and F. Totti, *J. Mater. Chem. C*, 2015, **3**, 7294.
13 M. Telychko, J. Su, A. Gallardo, Y. Gu, J. I. Mendieta-Moreno, D. Qi, A. Tadich, S. Song, P. Lyu, Z. Qiu, H. Fang, M. J. Koh, J. Wu, P. Jelínek and J. Lu, *Angew. Chem., Int. Ed.*, 2019, **58**, 18591.
14 W. Auwärter, D. Ecija, F. Klappenberger and J. V. Barth, *Nat. Chem.*, 2015, **7**, 105.
15 J. M. Gottfried, *Surf. Sci. Rep.*, 2015, **70**, 259.
16 H. Marbach, *Acc. Chem. Res.*, 2015, **48**, 2649.
17 T. E. Shubina, H. Marbach, K. Flechtner, A. Kretschmann, N. Jux, F. Buchner, H.-P. Steinrück, T. Clark and J. M. Gottfried, *J. Am. Chem. Soc.*, 2007, **129**, 9476.
18 G. Mette, D. Sutter, Y. Gurdal, S. Schnidrig, B. Probst, M. Iannuzzi, J. Hutter, R. Alberto and J. Osterwalder, *Nanoscale*, 2016, **8**, 7958.
19 G. Kresse and J. Furthmüller, *Comput. Mater. Sci.*, 1996, **6**, 15.
20 G. Kresse and J. Furthmüller, *Phys. Rev. B: Condens. Matter Mater. Phys.*, 1996, **54**, 11169.
21 P. E. Blochl, *Phys. Rev. B: Condens. Matter Mater. Phys.*, 1994, **50**, 17953.
22 G. Kresse and D. Joubert, *Phys. Rev. B: Condens. Matter Mater. Phys.*, 1999, **59**, 1758.
23 J. P. Perdew, K. Burke and M. Ernzerhof, *Phys. Rev. Lett.*, 1996, **77**, 3865; *Phys. Rev. Lett.*, 1997, **78**, 1396.
24 S. Grimme, J. Antony, S. Ehrlich and H. Krieg, *J. Chem. Phys.*, 2010, **132**, 154104.
25 J. P. Perdew and M. Ernzerhof, *J. Chem. Phys.*, 1996, **105**, 9982.
26 W. Tang, E. Sanville and G. Henkelman, *J. Phys.: Condens. Matter*, 2009, **21**, 084204.
27 M. J. Frisch, *et al.*, *Gaussian 09*, Revision D.01, Wallingford CT, 2009.
28 B3P86 functional is defined by its implementation in the Gaussian program.
29 P. J. Stephens, F. J. Devlin, C. F. Chabalowski and M. J. Frisch, *J. Phys. Chem.*, 1994, **98**(45), 11623.
30 B. de la Torre, M. Švec, P. Hapala, J. Redondo, O. Krejčí, R. Lo, D. Manna, A. Sarmah, D. Nachtigallová, J. Tuček, P. Błoński, M. Otyepka, R. Zbořil, P. Hobza and P. Jelínek, *Nat. Commun.*, 2018, **9**, 2831.
31 K. Kaiser, L. Gross and F. Schulz, *ACS Nano*, 2019, **13**, 6947.
32 J. Kestell, J. Walker, Y. Bai, J. A. Boscoboinik, M. Garvey and W. T. Tysoe, *J. Phys. Chem. C*, 2016, **120**(17), 9270.
33 Y. Feng, L. Liu, J.-T. Wang, H. Huang and Q.-X. Guo, *J. Chem. Inf. Comput. Sci.*, 2003, **43**, 2005.
34 P. Trouillas, P. Marsal, D. Siri, R. Lazzaroni and J.-L. Duroux, *Food Chem.*, 2006, **97**, 679.
35 B. Cirera, B. de la Torre, D. Moreno, M. Ondráček, R. Zbořil, R. Miranda, P. Jelínek and D. Écija, *Chem. Mater.*, 2019, **31**, 3248.